



**Fermi National Accelerator Laboratory**

**FERMILAB-Pub-92/124**

# **Analytical Evaluation of the Second Order Momentum Compaction Factor and Comparison with MAD Results**

J.P. Shan, S.G. Peggs, S.A. Bogacz

*Fermi National Accelerator Laboratory  
P.O. Box 500, Batavia, Illinois 60510*

April 1992

Submitted to *Particle Accelerators*

## **Disclaimer**

*This report was prepared as an account of work sponsored by an agency of the United States Government. Neither the United States Government nor any agency thereof, nor any of their employees, makes any warranty, express or implied, or assumes any legal liability or responsibility for the accuracy, completeness, or usefulness of any information, apparatus, product, or process disclosed, or represents that its use would not infringe privately owned rights. Reference herein to any specific commercial product, process, or service by trade name, trademark, manufacturer, or otherwise, does not necessarily constitute or imply its endorsement, recommendation, or favoring by the United States Government or any agency thereof. The views and opinions of authors expressed herein do not necessarily state or reflect those of the United States Government or any agency thereof.*

# ANALYTICAL EVALUATION OF THE SECOND ORDER MOMENTUM COMPACTION FACTOR AND COMPARISON WITH MAD RESULTS

J.P. SHAN and S.G. PEGGS and S.A. BOGACZ

*Fermi National Accelerator Laboratory\*, P.O. Box 500, Batavia, IL 60510*

The second order momentum compaction factor  $\alpha_1$  is a critical lattice parameter for transition crossing in hadron synchrotrons and for the operation of quasi-isochronous storage rings, which have been proposed for free electron lasers, synchrotron light sources and recently for high luminosity  $e^+e^-$  colliders. First the relation between the momentum compaction factor and the dispersion function is established, with the "wiggling effect" included. Then an analytical expression of  $\alpha_1$  is derived for an ideal FODO lattice by solving the differential equation for the dispersion function. A numerical calculation using MAD is performed to show excellent agreement with the analytical result. Finally, a more realistic example, the Fermilab Main Injector, is also considered.

KEY WORDS: Momentum Compaction, Dispersion Function

## 1 INTRODUCTION

In a synchrotron or storage ring, particles with different momenta have different closed orbits. The difference in the closed orbit length ( $\Delta C$ ) between a particle with momentum  $p$  and a reference particle with momentum  $p_0$  may be expressed as an expansion in momentum offset  $\delta$

$$\Delta C = C_0 \alpha_0 \delta [1 + \alpha_1 \delta + O(\delta^2)], \quad (1)$$

where  $C_0$  is the length of the reference orbit, and

$$\delta = \frac{p - p_0}{p_0} = \frac{\Delta p}{p_0}. \quad (2)$$

Such a dependence of orbit length on momentum is called momentum compaction, and  $\alpha_0$  is the linear momentum compaction factor. The second order momentum compaction factor  $\alpha_1$  is the focus of this paper.

---

\* Operated by the Universities Research Association Inc., under contract with the U.S. Department of Energy.

Although rooted in the transverse motion, the momentum compaction effect influences the longitudinal motion through the phase slip factor

$$\eta = \frac{1}{T_0} \frac{T - T_0}{\delta} = \eta_0 + \eta_1 \delta + O(\delta^2), \quad (3)$$

where

$$\eta_0 = \alpha_0 - \frac{1}{\gamma^2} \equiv \frac{1}{\gamma_T^2} - \frac{1}{\gamma^2}, \quad (4)$$

$$\eta_1 = \alpha_0 \alpha_1 + \frac{3\beta^2}{2\gamma^2} - \frac{\eta_0}{\gamma^2}. \quad (5)$$

Here  $T$  is the period of revolution for a particle with momentum offset  $\delta$  and  $T_0$  is for a synchronous particle,  $\beta$  and  $\gamma$  follow usual relativistic kinematic notation, and  $\gamma_T$  is the transition gamma for a synchronous particle. For a conventional FODO lattice  $\gamma_T$  is roughly equal to the horizontal tune of the machine, which is about  $5 \sim 30$  depending on the size of machine. So, most of the medium energy hadron synchrotrons have to cross transition. Near transition  $\eta$  and  $\eta_0$  are small and the contribution from the nonlinear term

$$\eta_1 \approx \alpha_0 \left( \alpha_1 + \frac{3}{2} \right) \quad (6)$$

becomes very important. Nonzero  $\eta_1$  leads to the fact that higher momentum particles and lower momentum particles can not agree when the synchronous phase should be switched <sup>1</sup>. In reality the phase switch can only happen at one particular instant, so most particles have to experience a defocusing radio frequency (RF) force for a period of time. This may be the dominant mechanism causing emittance blow-up and possibly beam loss for some machines, according to tracking studies <sup>234</sup> and a preliminary experiment <sup>5</sup>. If we can set  $\alpha_1 = -1.5$ , the nonlinear effect will be suppressed and transition crossing will become much less harmful.

All electron machines operate well above transition, or  $\gamma \gg \gamma_T$ , so

$$\eta_0 \approx \alpha_0, \quad \eta_1 \approx \alpha_0 \alpha_1. \quad (7)$$

While the bunch length is roughly proportional to  $\sqrt{\eta_0}$ , it may be possible to get very short bunches by using quasi-isochronous rings with very small  $\alpha_0$  values. These have been proposed for free electron laser drivers <sup>6</sup>, for synchrotron light sources <sup>7</sup> and for the next generation of high luminosity  $e^+e^-$  colliders <sup>8</sup>. There, the momentum acceptance of the RF bucket, which goes roughly like  $\eta_0/\eta_1$  (or  $\alpha_1^{-1}$ ), should be larger than 10 times the root mean square momentum spread of bunch  $\delta_{rms}$  in order to preserve reasonable quantum life time. That is

$$\alpha_1 < \frac{1}{10\delta_{rms}}. \quad (8)$$

If  $\delta_{rms} = 6 \times 10^{-4}$ , a value of  $\alpha_1$  smaller than 170 is required, which is not necessarily easy to get since  $\alpha_0$  itself is very small.

The above comments suggest that  $\alpha_1$  is a very important lattice parameter which has to be controlled in the small  $\eta$  regime. Next we turn to establish the relation between the momentum compaction factor and the dispersion function, with the “wiggling effect” included.

## 2 THE WIGGLING FACTOR

To describe the closed orbit  $x_{co}(s, \delta)$  of an off-momentum particle, the dispersion function is introduced as

$$D(s, \delta) = \frac{x_{co}(s, \delta) - x_{co}(s, 0)}{\delta} = D_0(s) + D_1(s)\delta + O(\delta^2), \quad (9)$$

where  $x_{co}(s, 0)$  is the reference orbit, and  $s$  is the azimuthal coordinate. Usually we refer to  $D_0$ , the linear part of dispersion function, as the dispersion function because  $\delta \ll 1$ . Since we are interested in  $\alpha_1$ , the first nonlinear part  $D_1$  has also to be included. Furthermore the effect of closed orbit offset on  $\alpha_1$  is negligible (Appendix A), therefore we can assume  $x_{co}(s, 0) = 0$ .

Now, consider an infinitesimal piece of arc shown schematically in Fig. 1, where the orbit length of a synchronous particle (AA') is  $ds = \rho d\theta$  and  $\rho$  is the radius of curvature. Then a particle with momentum offset  $\delta$  will follow the orbit BB' with length

$$dl_2 = dl_1 \sqrt{1 + (D'_0 \delta)^2} = ds \left[ 1 + \frac{D_0}{\rho} \delta + \left( \frac{D_1}{\rho} + \frac{1}{2} D_0'^2 \right) \delta^2 \right], \quad (10)$$

rather than

$$dl_1 = (\rho + D_0 \delta + D_1 \delta^2) d\theta = ds \left[ 1 + \frac{D_0}{\rho} \delta + \frac{D_1}{\rho} \delta^2 \right], \quad (11)$$

where  $D'_0 = \frac{dD_0}{ds}$ . Notice the difference of  $dl_2$  and  $dl_1$  in second order, which is called the “wiggling effect”. This relation is also valid for a straight sector if the limit  $\rho \rightarrow \infty$  is taken in the appropriate way. There, the only difference in orbit length is due to the “wiggling effect”.

The difference in total closed orbit length of an off-momentum particle from that of a reference particle is simply

$$\Delta C = \oint (dl_2 - ds) = \oint \alpha_0 (\delta + \alpha_1 \delta^2) ds. \quad (12)$$

Comparison of Eq.(1) and Eq. (12) yields

$$\alpha_0 = \frac{1}{C_0} \oint \frac{D_0}{\rho} ds \equiv \left\langle \frac{D_0}{\rho} \right\rangle \quad (13)$$

and

$$\alpha_1 = \frac{\langle D_1/\rho \rangle}{\alpha_0} + \frac{\langle D_0'^2 \rangle}{2\alpha_0}, \quad (14)$$

where  $C_0 = \oint ds$  and  $\langle \dots \rangle$  means the average in the whole ring, and the last term in Eq. (14) is called the wiggling factor <sup>9</sup>

$$w = \frac{1}{2\alpha_0} \langle D_0'^2 \rangle = \frac{\langle D_0'^2 \rangle}{2\langle D_0/\rho \rangle}. \quad (15)$$

This term is missing from some references, but will be shown to have significant contribution to  $\alpha_1$ .

Betatron oscillations may also contribute to the difference in orbit length (and thus  $\alpha_1$ ). In general, this effect is very small.

### 3 DIFFERENTIAL EQUATIONS FOR THE DISPERSION FUNCTION

Motion in a circular accelerator is conveniently represented by the Hamiltonian (with azimuthal coordinate  $s$  instead of time  $t$  as independent variable) <sup>10</sup>

$$\begin{aligned} H = -p_s &= -\frac{eA_s}{c} - \left(1 + \frac{x}{\rho}\right)p \left[1 - \left(\frac{p_x}{p}\right)^2 - \left(\frac{p_y}{p}\right)^2\right]^{1/2} \\ &\approx -\frac{eA_s}{c} - \left(1 + \frac{x}{\rho}\right)p \left[1 - \frac{1}{2}\left(\frac{p_x}{p}\right)^2 - \frac{1}{2}\left(\frac{p_y}{p}\right)^2\right], \end{aligned} \quad (16)$$

where the canonical vector potential

$$A_s = -\frac{p_0 c}{e} \left[ \frac{x}{\rho} + \left(\frac{1}{\rho^2} - K_1\right) \frac{x^2}{2} + \frac{K_1 y^2}{2} + \frac{1}{6} K_2 (x^3 - 3xy^2) \right], \quad (17)$$

for a lattice composed of separated-function magnets with hard edge. Here  $K_1$  and  $K_2$  are respectively the quadrupole and the sextupole strength for a reference particle

$$K_1 = \frac{e}{p_0 c} \frac{\partial B_y}{\partial x}, \quad K_2 = \frac{e}{p_0 c} \frac{\partial^2 B_y}{\partial x^2},$$

The canonical differential equations of motion are obtained by partial differentiation of  $H$ , which are expanded to become

$$x' = \frac{\partial H}{\partial p_x} = \left(1 + \frac{x}{\rho}\right) \frac{p_x}{p}, \quad (18)$$

$$p_x' = -\frac{\partial H}{\partial x} = -p_0 \left(\frac{1}{\rho^2} - K_1\right)x + \frac{p - p_0}{\rho} + \frac{p_0 x'^2}{2\rho} - \frac{p_0}{2} K_2 (x^2 - y^2), \quad (19)$$

where the prime represents the differentiation with respect to  $s$ , the azimuthal coordinate. Combining Eq.(18) and Eq.(19) we get the equation of motion

$$x'' + \left(1 + \frac{x}{\rho}\right) \frac{1}{1 + \delta} \left(\frac{1}{\rho^2} - K_1\right)x = \left(1 + \frac{x}{\rho}\right) \frac{\delta}{1 + \delta} \frac{1}{\rho} + \frac{x'^2}{2\rho} - \frac{1}{2} K_2 (x^2 - y^2), \quad (20)$$

which is exact to order  $\delta^2$ . Substituting  $x = D_0\delta + D_1\delta^2$  and  $y = 0$  yields

$$D_0'' + \left(\frac{1}{\rho^2} - K_1\right)D_0 = \frac{1}{\rho}, \quad (21)$$

$$D_1'' + \left(\frac{1}{\rho^2} - K_1\right)D_1 = \frac{D_0'^2}{2\rho} - K_1D_0 - \frac{1}{\rho} \left(1 - \frac{D_0}{\rho}\right)^2 - \frac{1}{2}K_2D_0^2. \quad (22)$$

These inhomogenous Hill equations could be solved in principle by using Green's function <sup>11</sup>. But it is not obvious to see how the dispersion function is related to other lattice parameters. In the next section we will solve Eq. (21) and Eq. (22) explicitly for an ideal FODO lattice, which is not far away from some realistic lattices, as shown later.

#### 4 A SOLUBLE CASE: THE IDEAL FODO LATTICE

The ideal FODO lattice that we consider is composed of N identical FODO cells, or 2N half cells. Each half cell (Fig. 2) starts at the center of a thin focussing quadrupole (QF) and ends at the center of a neighboring thin defocussing quadrupole (QD). The absolute integrated strength of half QF and QD is the same

$$q = |K_1|l_{hQ} = \frac{1}{f},$$

where  $K_1$  is the quadrupole gradient, and  $l_{hQ}$  and  $f$  are respectively the physical length and the focal length of the half quadrupole. The bending angle of each dipole is

$$\theta_0 = \frac{\pi}{N} = \frac{L}{R},$$

where L is the half cell length, or the length of each dipole since  $l_{hQ} \rightarrow 0$ , and R is the radius of curvature for the reference particle. Another characteristic parameter is

$$s = qL \approx \sin \phi_{1/2}, \quad (23)$$

which should not be confused with azimuthal coordinate s, where  $\phi_{1/2}$  is the betatron phase advance per half cell. It seems that one only needs to solve Eq.(21) and Eq.(22) in the dipole. Actually the necessary boundary conditions have also to be imposed by the thin quadrupoles.

In the dipole ( $\rho = R$  and  $K_1 = 0$ ), Eq.(21) reduces to

$$D_{0B}'' + \frac{1}{R^2}D_{0B} = \frac{1}{R}, \quad (24)$$

which is equivalent to

$$\ddot{D}_{0B} + D_{0B} = R, \quad (25)$$

where a dot represents the differentiation with respect to  $\theta$ . The general solution of Eq.(25) is

$$D_{0B}(\theta) = R(1 + c_1 \sin \theta + c_2 \cos \theta). \quad (26)$$

In a quadrupole, Eq.(21) reduces to

$$D_{0Q}'' - K_1 D_{0Q} = 0, \quad (27)$$

which provides the boundary conditions

$$D_{0Q}'(\pm \frac{\theta_0}{2}) = -q D_{0Q}(\pm \frac{\theta_0}{2}). \quad (28)$$

Here use has been made of the symmetry condition  $D_{0Q}' = 0$  at the center of the quadrupoles.

The continuity of  $D$  and  $\frac{dD}{dl_2}$

$$\frac{dD}{dl_2} = (1 + \frac{x}{\rho})^{-1} \frac{dD}{ds} = (1 + \frac{x}{\rho})^{-1} D' \quad (29)$$

yields

$$\dot{D}_{0B}(\pm \frac{\theta_0}{2}) = R D_{0Q}'(\pm \frac{\theta_0}{2}) = -Q D_{0B}(\pm \frac{\theta_0}{2}), \quad (30)$$

$$\dot{D}_{1B}(\pm \frac{\theta_0}{2}) = R D_{1Q}'(\pm \frac{\theta_0}{2}) + D_0(\pm \frac{\theta_0}{2}) D_{0Q}'(\pm \frac{\theta_0}{2}), \quad (31)$$

where

$$Q = Rq = \frac{s}{\theta_0} = \frac{Ns}{\pi}. \quad (32)$$

Substituting

$$\dot{D}_{0B}(\theta) = R(c_1 \cos \theta - c_2 \sin \theta) \quad (33)$$

into Eq.(30), we arrive after some algebra at the solution

$$c_1 = \frac{c_2}{Q} = -\frac{Q}{(1 + Q^2) \cos \frac{\theta_0}{2}}. \quad (34)$$

With the aid of Eq.(34), Eq.(26) and Eq.(33) can be rewritten as

$$D_{0B}(\theta) = R[1 + c_1(\sin \theta + Q \cos \theta)], \quad (35)$$

$$\dot{D}_{0B}(\theta) = R c_1(\cos \theta - Q \sin \theta). \quad (36)$$

Substituting Eq.(35) into Eq.(13) and Eq.(15) gives

$$\alpha_0 = \frac{1}{\theta_0} \int_{-\frac{\theta_0}{2}}^{+\frac{\theta_0}{2}} d\theta \frac{D_{0B}}{R} = 1 + c_2 \frac{2 \sin \frac{\theta_0}{2}}{\theta_0} = 1 - \frac{2tQ^2}{\theta_0(1 + Q^2)}, \quad (37)$$

where  $t = \tan(\frac{1}{2}\theta_0)$ , and the wiggling factor

$$w = \frac{\langle D_0'^2 \rangle}{2\alpha_0} = \frac{Q^2 [\theta_0(1+t^2)(1+Q^2) + 2t(1-Q^2)]}{4(1+Q^2)[\theta_0(1+Q^2) - 2tQ^2]}. \quad (38)$$

The relationships

$$\sin \theta_0 = \frac{2t}{1+t^2}, \quad \cos \theta_0 = \frac{1-t^2}{1+t^2} \quad (39)$$

have been used to simplify the result.

Following the same procedure, we now solve  $D_1$ . In the dipole

$$D_{1B}'' + \frac{1}{R^2}D_{1B} = -\frac{1}{R}\left(\frac{D_{0B}}{R} - 1\right)^2 + \frac{1}{R}\frac{D_{0B}'^2}{2} \quad (40)$$

with the general solution

$$D_{1B}(\theta) = R[c_3 \sin \theta + c_4 \cos \theta] - R \left[ \frac{1}{4}c_1^2(1+Q^2) + \frac{1}{4}c_1^2(1-Q^2) \cos 2\theta - \frac{1}{2}Qc_1^2 \sin 2\theta \right]. \quad (41)$$

Before solving the equation, notice

$$D_{1B}(\theta) = R[c_3 \sin \theta + c_4 \cos \theta] - \frac{1}{2R}\dot{D}_{0B}^2, \quad (42)$$

which leads to a very simple closed result

$$\alpha_0 \alpha_1 = \frac{1}{\theta_0} \int_{-\frac{\theta_0}{2}}^{+\frac{\theta_0}{2}} d\theta \left( \frac{D_{1B}}{R} + \frac{1}{2R^2}\dot{D}_{0B}^2 \right) = c_4 \frac{2 \sin \frac{\theta_0}{2}}{\theta_0}. \quad (43)$$

To find  $\alpha_1$ , we now only need to calculate  $c_4$ . Let's proceed with Eq.(22) in the thin quadrupole

$$D_{1Q}'' - K_1 D_{1Q} = -K_1 D_{0Q}, \quad (44)$$

which leads to

$$D_{1Q}'(\pm \frac{\theta_0}{2}) = -q [D_{1Q}(\pm \frac{\theta_0}{2}) - D_{0Q}(\pm \frac{\theta_0}{2})]. \quad (45)$$

With Eq.(31), the boundary conditions become

$$D_{1B}'(\pm \frac{\theta_0}{2}) = -Q \left[ D_{1B}(\pm \frac{\theta_0}{2}) - D_{0B}(\pm \frac{\theta_0}{2}) + \frac{D_{0B}'^2(\pm \frac{\theta_0}{2})}{R} \right]. \quad (46)$$

By solving Eq.(46) we find

$$c_4 = \frac{Q^4(Q^2 t^2 + 3)}{2 \cos \frac{\theta_0}{2} (1+Q^2)^3}. \quad (47)$$

Substituting Eq.(47) into Eq.(43) we have

$$\alpha_0\alpha_1 = \frac{Q^4t(Q^2t^2 + 3)}{\theta_0(1 + Q^2)^3}. \quad (48)$$

Further substitution of Eq.(37) into Eq.(48) allows one to write

$$\alpha_1 = \frac{Q^4t(Q^2t^2 + 3)}{(1 + Q^2)^2 [\theta_0(1 + Q^2) - 2tQ^2]}, \quad (49)$$

which could alternatively be expressed as a function of  $s$

$$\alpha_1 = \frac{s^4t(s^2t^2 + 3\theta_0^2)}{(\theta_0^2 + s^2)^2 [\theta_0(\theta_0^2 + s^2) - 2ts^2]}. \quad (50)$$

This result was also independently reached through a geometric approach<sup>12</sup>.

Notice that both  $w$  and  $\alpha_1$  only depend on the strength of the quadrupoles and the number of cells. Fig. 3 and Fig. 4 are respectively plots of  $w$  and  $\alpha_1$  as a function of  $s$  with different number of cells. For a given  $N$ ,  $w$  and  $\alpha_1$  increase as quadrupoles become stronger. The possible value of  $s$  is somewhere between 0 and 1 since  $s \approx \sin \phi_{\frac{1}{2}}$ . In the case  $s = 0$  (cyclotron), from Eq. (37) and Eq. (49) we have  $\alpha_0 = 1$  and  $\alpha_1 = 0$  as expected. Actually we can show from symmetry that  $\alpha_n (n \geq 1) = 0$ . For real synchrotrons  $\phi_{\frac{1}{2}}$  is usually between 30 and 45 degrees, and the operating range for  $s$  is  $0.5 \sim 0.7$ . Also notice that  $w$  and  $\alpha_1$  increase with  $N$ . Since  $N$  increases as ring size (roughly  $N \propto \sqrt{R}$ ),  $w$  and  $\alpha_1$  are bigger for larger machines.

In the case  $N \rightarrow \infty$ , the centrifugal focussing of dipoles becomes negligible, and the analytical results reduce to

$$\alpha_0 = \frac{1}{Q^2} \left( 1 - \frac{s^2}{12} \right), \quad (51)$$

$$w = \frac{1 + \frac{s^2}{12}}{2 \left( 1 - \frac{s^2}{12} \right)}, \quad (52)$$

$$\alpha_1 = \frac{3 \left( 1 + \frac{s^2}{12} \right)}{2 \left( 1 - \frac{s^2}{12} \right)} = 3w. \quad (53)$$

## 5 COMPARISON WITH MAD

In general, the differential equations cannot be solved analytically and numerical method has to be used. Unfortunately,  $\alpha_1$  is not directly available from the general codes such as MAD<sup>13</sup>, which instead return the momentum compaction factor  $\alpha_p$ . The value of  $\alpha_1$  has to be extracted from the dependence of  $\alpha_p$  on  $\delta$ . Care must be taken about which definition of  $\alpha_p$  is used in a specific code. It may be

$$\alpha_{p1} = \frac{p}{C} \frac{dC}{dp} = \alpha_0 \left[ 1 + 2(\alpha_1 + \frac{1}{2} - \frac{1}{2}\alpha_0)\delta \right] + O(\delta^2), \quad (54)$$

or

$$\alpha_{p2} = \frac{p_s}{C_s} \frac{dC}{dp} = \alpha_0(1 + 2\alpha_1\delta) + O(\delta^2), \quad (55)$$

or something else. It is also important to test these codes using some very simple lattices, for which an analytical solution is possible. If there is a good agreement, we can have confidence in numerical solutions of realistic lattices such as the Main Ring or the Main Injector, or an isochronous ring.

A lattice composed of 80 simplified FODO cells was set up as input to MAD. The length of a quadrupole was chosen as 1 micron. For every  $s$ , the momentum compaction factor  $\alpha_p$  is calculated by MAD at three momentum offsets  $\delta = -0.001, 0, +0.001$ . Then  $\alpha_1$  was extracted from  $\alpha_p$  depending upon the definition of  $\alpha_p$ , either

$$\alpha_1 = \frac{\alpha_{p1}(\delta) - \alpha_{p1}(-\delta)}{4\alpha_0\delta} - \frac{1}{2} + \frac{\alpha_0}{2}, \quad (56)$$

if  $\alpha_p = \alpha_{p1}$ , or

$$\alpha_1 = \frac{\alpha_{p2}(\delta) - \alpha_{p2}(-\delta)}{4\alpha_0\delta}, \quad (57)$$

if  $\alpha_p = \alpha_{p2}$ . If we use the first definition, a large disagreement occurs between the MAD result and the theoretical prediction from Eq.(49). However, excellent agreement is achieved using the second definition, as shown in Fig. 5. The systematic discrepancy found in ref. <sup>14</sup> is now understood.

## 6 DEVIATION FROM THE IDEAL FODO LATTICE

Taking the Main Injector ( $N = 80, s = \sin \frac{\pi}{4} = \frac{1}{\sqrt{2}}$ )<sup>15</sup> as an example, we will see how the deviations from an ideal FODO lattice affect  $\alpha_1$ .

### 6.1 Sector Dipoles and Rectangular Dipoles

In the ideal lattice we assumed there was no dipole edge focussing, as with sector dipoles. In reality the Main Injector dipole is rectangular. How important is this? Fig. 5 shows that the difference between sector dipoles and rectangular dipoles is negligible in the case of Main Injector. But as the cell phase advance and/or number of cells decreases the edge focussing becomes more important. So special care has to be taken with edge focussing in small accelerator rings.

### 6.2 Finite Length Quadrupole

For the simplicity of analytical solution, we have used a thin quadrupole approximation. What happens if quadrupole has finite length? From the MAD calculation

(Tab. 1), we see that the contribution of finite quadrupole length is also negligible. This is not a surprise because the dominant source of momentum compaction comes from dispersion in dipoles, and the boundary conditions are dominated by the integrated strength of the quadrupoles.

TABLE 1: The dependence of  $\alpha_1$  on the half quadrupole length

Half Quadrupole Length $l_Q$ (m)	$1 \times 10^{-6}$	0.1	0.5
$\alpha_1$	1.545	1.546	1.550

### 6.3 Contribution from Sextupoles

Because of the head-tail instability, the natural chromaticity is usually compensated by sextupoles. If the sextupole strengths are set to make the net chromaticity  $1 - f$  times the natural chromaticity,  $D_0$  (and thus  $\alpha_0$  and  $w$ ) will not change while  $D_1$  will be modified, as shown in <sup>14</sup>

$$\langle D_1 \rangle \approx \frac{R}{Q^2} \left( 1 - f + \frac{s^2}{12} \right). \quad (58)$$

This approximation is true when the focussing from dipoles is negligible. Then

$$\alpha_1 = \frac{3 - 2f + \frac{s^2}{4}}{2 \left( 1 - \frac{s^2}{12} \right)}. \quad (59)$$

So, when the net chromaticity is compensated to zero, or  $f = 1$ ,

$$0.5 \leq \alpha_1 = \frac{1 + \frac{s^2}{4}}{2 \left( 1 - \frac{s^2}{12} \right)} \leq .68, \quad (60)$$

because  $0 \leq s \leq 1$ . For the Main Injector  $s^2 = 0.5$ , and we have  $\alpha_1 = 0.587$ . A value of  $\alpha_1 = -1.5$  can be obtained in principle by setting

$$f \approx 3, \quad (61)$$

resulting in unpleasantly strong nonlinear fields.

## 7 CONCLUSION AND DISCUSSION

Starting with a Hamiltonian, we derived the differential equation for the two leading terms in the dispersion function, which is exact for any lattice composed of separated-function magnets with hard edge. The linear term  $D_0$  is determined only by linear elements (dipoles and quadrupoles). The first nonlinear correction  $D_1$  also depends on sextupoles, but not on octupoles or higher order magnets.

For an ideal FODO lattice, the differential equations were solved to get analytical expressions for  $\alpha_0$ ,  $w$  and  $\alpha_1$ . A comparison with MAD calculations of momentum compaction factor showed perfect agreement. Then MAD was used to show that conventional FODO-like lattices are not far away from the ideal one. In a large machine such as the Fermilab Main Injector, we found that  $\alpha_1$  is not sensitive to quadrupole length and edge focussing.

## ACKNOWLEDGEMENTS

The possible importance of the previously neglected wiggling factor was first pointed out to us by Leo Michelotti. We thank K.Y. Ng for his help in the discussion of differential equations. Discussions with W. Gabella were also very fruitful. Thanks also go to C. Ankenbrandt for his comments.

## REFERENCES

1. K. Johnsen. In *Proc. of the CERN Symposium on High Energy Accelerators and Pion Physics*, pages 106–109, CERN, 1956.
2. J. Wei. *Longitudinal Dynamics of the Non-Adiabatic Regime on Alternating-Gradient Synchrotrons*. Ph.D. dissertation, State University of New York at Stony Brook, May 1990.
3. S.A. Bogacz. In *Proceedings of the Fermilab III Instabilities Workshop*, page 116, Fermilab, June 1990.
4. I. Kourbanis and K.Y. Ng. In *Proceedings of the Fermilab III Instabilities Workshop*, pages 141–150, Fermilab, June 1990.
5. I. Kourbanis. In *Proceedings of IEEE Particle Accelerator Conference*, page 1292, San Francisco, 1991.
6. D.A.G. Deacon. *Physics Report*, 76(5):349–391, 1981.
7. S. Chattopadhyay et al. In *Proceedings of ICFA workshop on low emittance  $e^-e^+$  beams*, BNL 52090, 1987.
8. C. Pellegrini and D. Robin. *Nucl.Instr.and Meth. A*, 301:27–36, 1991.
9. E. Ciapala, A.Hofmann, S. Myers, and T. Risselada. *IEEE Nul.*, 26(3), June 1979.
10. E.D. Courant and H.S. Snyder. *Ann. of Phys*, 3:1, 1958.
11. J.-P. Delahaye and J. Jager. *Particle Accelerator*, 18:183–201, 1986.
12. K.Y. Ng. Higher-order momentum compaction for a simplified FODO lattice and comparison with SYNCH. Fermilab FN 578, December 1991.
13. H. Grote and F.C. Iselin. *The MAD Program(Methodical Accelerator Design), User's Reference Manual*. CERN, 8.1 edition, September 1990.
14. S.A. Bogacz and S. G. Peggs. In *Proceedings of the Fermilab III Instabilities Workshop*, pages 192–206, Fermilab, June 1990.
15. Fermilab Main Injector. Conceptual design report revision 2.3, Addendum, Fermilab, March 1991.

APPENDIX A THE EFFECT OF CLOSED ORBIT OFFSET ON  $\alpha_1$ 

In section 2 we assume that closed reference orbit is flat,  $x_{co} = 0$ . Actually there is always a closed orbit offset due to various errors. Since such an offset  $x_{co}$  is comparable to  $D\delta$ , it is natural to ask if it will affect the calculation of  $\alpha_1$ . The answer is that this effect is negligible for any realistic orbit offset.

For mathematical convenience, consider a simple model lattice, where the undistorted closed orbit is a circle with radius  $R$ . Now, if the distorted closed orbit for a reference particle is  $x_{co}(s)$ , its circumference will be

$$C_0 = 2\pi R \left( 1 + \frac{\langle x_{co} \rangle}{R} + \frac{1}{2} \langle x_{co}'^2 \rangle \right), \quad (62)$$

where  $\langle x \rangle = \frac{1}{2\pi R} \oint x ds$ . The closed orbit length of a particle with momentum offset  $\delta$  is

$$C = 2\pi R \left[ 1 + \frac{\langle x_{co}(\delta) \rangle}{R} + \frac{1}{2} \langle x_{co}'^2(\delta) \rangle \right], \quad (63)$$

where

$$x(\delta)_{co} = x_{co} + D_0\delta + D_1\delta^2. \quad (64)$$

If Eq.(63) is reorganized into an expansion of  $\delta$  with the aid of Eq.(62) and compared to Eq.(1), we get

$$\alpha_0 = \frac{\frac{\langle D_0 \rangle}{R} + \langle x_{co}' D_0' \rangle}{1 + \frac{\langle x_{co} \rangle}{R} + \frac{1}{2} \langle x_{co}'^2 \rangle} \quad (65)$$

and

$$\alpha_1 = \frac{\frac{\langle D_1 \rangle}{R} + \frac{1}{2} \langle D_0'^2 \rangle + \langle x_{co}' D_1' \rangle}{\frac{\langle D_0 \rangle}{R} + \langle x_{co}' D_0' \rangle}. \quad (66)$$

Since the dispersion wave and the orbit offset wave have approximately the same wavelength (cell length), the effect of closed orbit offset on  $\alpha_1$  is negligible so long as  $x_{co} \ll D_0, D_1$ , which is always true in any practical case.

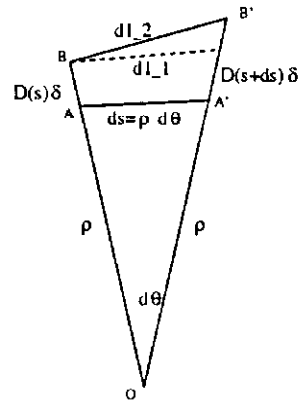


FIGURE 1: Schematic view of the wiggling effect

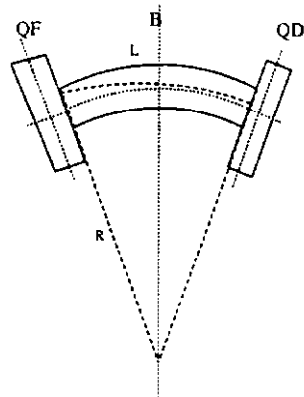


FIGURE 2: Schematic view of the half cell

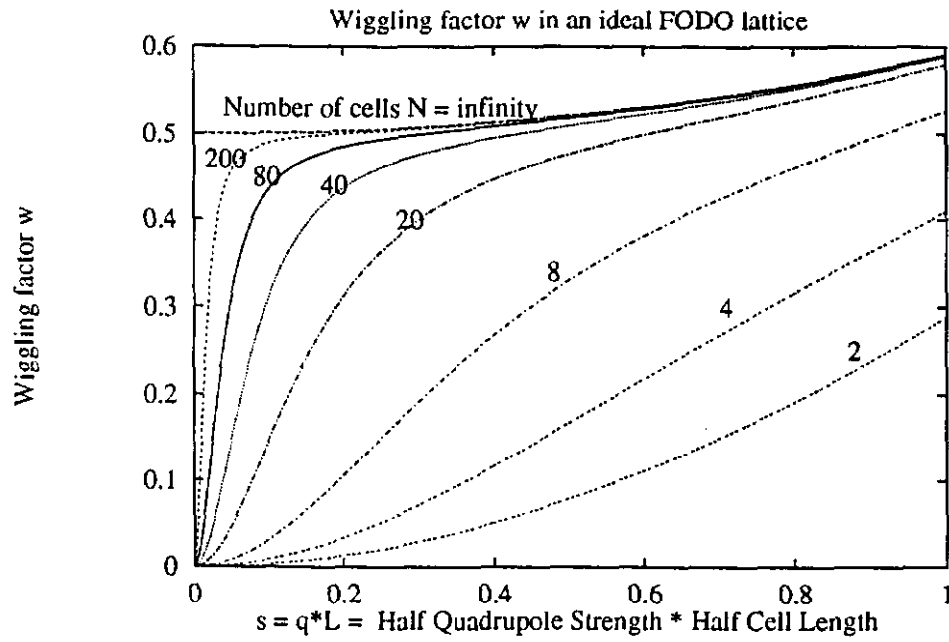


FIGURE 3: The wigging factor  $w$  as a function of  $s (\approx \sin \phi_{\frac{1}{2}})$  for different number of cells in an ideal FODO lattice.

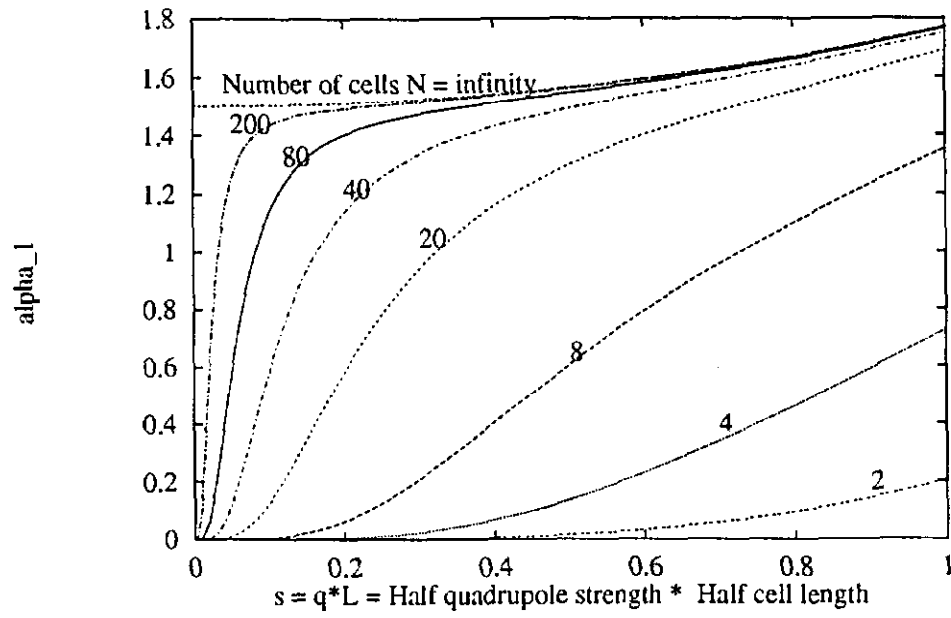


FIGURE 4:  $\alpha_1$  as a function of  $s (\approx \sin \phi_{\frac{1}{2}})$  with different number of cells in an ideal FODO lattice.

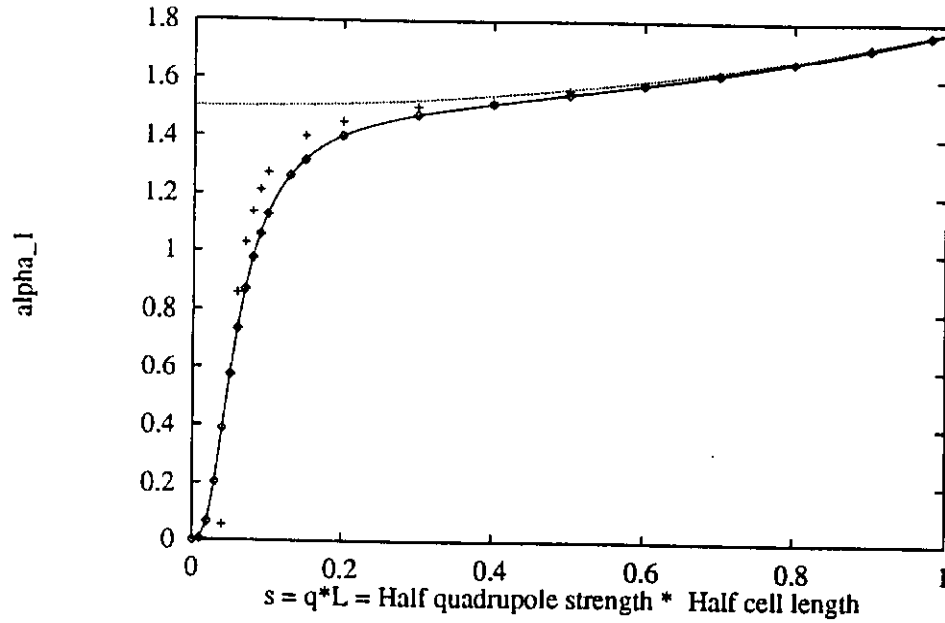


FIGURE 5: The comparison of  $\alpha_1$  calculated from MAD (diamond symbols) and predicted by the analytical expression (solid line) for an ideal FODO lattice with 80 cells (sector dipoles). The difference between the sector dipole case (diamond symbols) and the rectangular dipole case (plus symbols) becomes important in weak focussing machines. Also, one can see when the approximate formulae ( $N = \infty$ , dash line) begin to deviate from the exact result (solid line).